Strain-induced structural transformation of a silver nanowire

Mine Konuk[1] **and Sondan Durukanoğlu**[2,3]

[1] Department of Physics, Istanbul Technical University, Maslak, 34469 Istanbul, Turkey
[2] Faculty of Engineering and Natural Sciences, Sabanci University, Orhanli, Tuzla 34950 Istanbul, Turkey
[3] Nanotechnology Research and Application Center, Sabanci University, Orhanli, Tuzla 34950 Istanbul, Turkey

E-mail: sondan@sabanciuniv.edu

Received 19 January 2012, in final form 31 March 2012
Published 28 May 2012
Online at stacks.iop.org/Nano/23/245707

Abstract
We have investigated the structural characteristics of the experimentally observed phase transition of a silver nanowire into a tube under tensile strain. In the simulations, atoms are allowed to interact via a model potential extracted from the modified embedded atom method. Our calculations demonstrate that the formation of the hollow structure is governed by the nature of the applied strain, the length of the wire, and the initial cross-sectional shape. The results further offer insights into the atomistic nature of this specific structural transformation into a nanotube with the smallest possible cross-section.

S Online supplementary data available from stacks.iop.org/Nano/23/245707/mmedia

(Some figures may appear in colour only in the online journal)

1. Introduction

A recent high resolution transmission electron microscopy experiment has revealed the unprecedented structural transformation of a silver nanowire into a nanotube [1]. It was reported that upon application of an axial strain, the square nanometric bridges between the holes, that are delicately formed through electron bombardment on a self-supported silver thin film, can transform into a nanotube with the smallest possible cross-sectional area. In a follow up study, using *ab initio* density functional theory calculations Autreto *et al* also showed that the stability of these tubular structures is intrinsic and cannot be due to contamination of light atoms that might exist in the experimental set up [2]. It was recently reported that not only silver but also copper and gold nanowires undergo a similar structural transformation under a series of appropriate axial strains [3]. Such structural transformations are exciting because several applications in nano-mechanics and nano-tribology experiments involve nano-contacts that are under stretching. Nonetheless, the detailed atomistic mechanisms leading to the observed tubular structures are yet to be known. Also, although the non-equilibrium neck formations and their evolution under stretching have been well explored [4–7], this novel structural transformation from a wire to a nanotube is hardly in the scope of simulations.

In this paper, we present the results of our atomic-scale simulations to investigate the nature of the structural transformation from a silver nanowire to a nanotube using realistic calculations based on the interaction potentials extracted from the second nearest neighbor modified embedded atom method (2NN-MEAM) [8]. Due to the substantially increased compressive strain in the core of the wire, induced by the applied tensile strain along the length direction, the fcc wire undergoes a structural phase transition into a tubular wire, in a perfect agreement with the experimental observation [1]. Our simulations predict that this particular type of structural phase transformation is controlled by the nature of the applied strain, the length of the wire and the initial cross-sectional shape. Indeed, for such a perfect structural transformation, the ⟨100⟩ axially oriented fcc nanowire needs (1) to be formed by stacking A and B layers of an fcc crystal, both possessing the geometry of two interpenetrating one-lattice-parameter-wide squares, containing four atoms each (see figure 1(c)), (2) to have an optimum length of eight layers, and (3) to be exposed to a combination of low and high stress along the length direction.

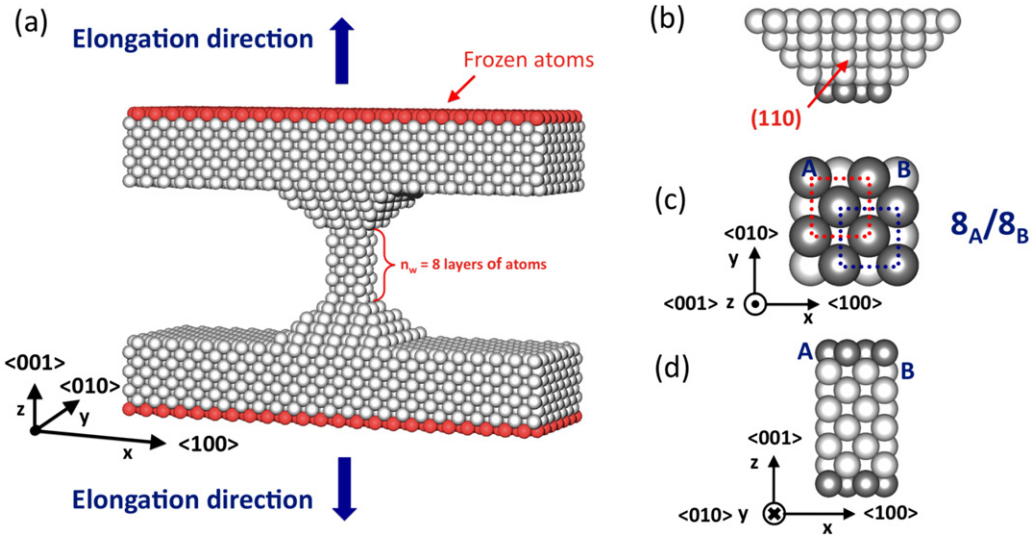

Figure 1. Computational cell for an eight-layer nanobridge. (a) Two silver thin films of eight layers are connected by a nanobridge through the pins. During the simulations, the red atoms at both the top and the bottom of the thin films are fixed. (b) Each pin with ⟨110⟩ surface skin orientations contains four layers of atoms along the axial direction and the darker layer belongs to the nanobridge. (c) The cross-sectional area with a 1.5 lattice parameter width contains eight atoms in each layer ($8_A/8_B$). (d) The side view of the ⟨100⟩ axially oriented nanobridge (eight layers in length).

2. Computational details and geometry

For systems with a high surface-to-volume ratio, the excessive unsaturated bondings are expected to play a crucial role in determining the equilibrium structure and thus a reliable definition of surface electron density is vital. The MEAM potentials are empirical extensions of the original EAM potentials [9] that include the directional bonding through the angular dependence of the atomic electron density [10]. The 2NN-MEAM, further, includes the second nearest-neighbor interactions and has proven to be reliable in correctly describing many characteristics of nano-structured materials [11–13]. In this work, we used the 2NN-MEAM potential to describe the interactions between the atoms in model systems and the parameters for the potential (for silver) were taken from table I in [8]; readers can refer to the same reference for precise values of parameters and relevant expressions.

The model systems for examining the strain-induced structural transformation are carefully chosen to mimic a more realistic description of experimentally generated nanowires. Hence, each computational cell is constructed to contain two silver thin films of eight layers that are connected by a nanobridge through the pins. In figure 1, we present the computational cell containing an eight-layer nanobridge between the pins. The total number of layers along the axial direction is 32—2 × 8 layers from the thin films at both ends, 2 × 4 from the pins and another eight layers from the nanobridge. The ⟨100⟩ axially oriented nanowire has a square cross-sectional area with a side of 1.5 lattice parameters and is formed by stacking of two different layers containing eight atoms ($8_A/8_B$) (figure 1(c)). Periodic boundary conditions are applied along the x and z directions and no such constraint is imposed along the y-direction to simulate a realistic thin film with a finite size.

Very briefly, in all the simulations the atoms in the computational cells were initially arranged in their perfect lattice positions in the truncated nanowire and allowed to interact via 2NN-MEAM potentials. Next, the standard conjugate gradient method was used to fully minimize the total energy of the system to eliminate non-zero initial stress. Once the equilibrated structures were attained, a series of strains was applied by stretching the wire along the axial direction. Each elongated system was then equilibrated while holding both the top and the bottom layers of the cell fixed.

3. Results and discussion

To examine the strain-induced structural phase transformation, the nanowires were exposed to two different strain regimes: a linear strain regime (uniform deformation) and a high-gradient strain regime (non-uniform deformation). In the linear strain regime a linearly varying displacement profile was imposed between the layers along the axial direction. In this regime, we conducted four different sets of simulations, corresponding to four incremental steps of 1, 2, 3, and 4 Å, to elongate the total length of the computational cell until the nanobridge at the middle was broken. In the simulations each elongation step was uniformly distributed to each layer separation in the system, thus leading to respective increments of 0.032 Å, 0.064 Å, 0.096 Å, 0.129 Å in the interlayer separation for 1 Å, 2 Å, 3 Å, and 4 Å incremental steps in the total length of the computational cell for the eight-layer nanobridge. On the other hand, in the high-gradient strain regime, the nanowires were exposed to a series of low and high stresses by simply varying the interlayer separations (i.e. the length of the computational cell) accordingly. In this regime, in each set of simulations the uniform elongation process—the successive and equivalent increment of the

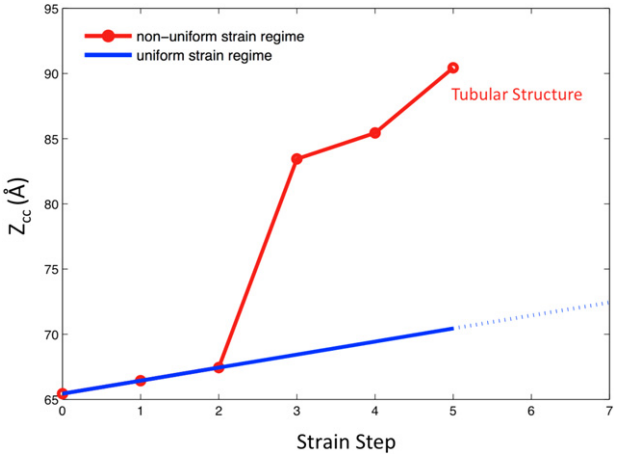

Figure 2. Examples of the sequential processes of elongation for both uniform and non-uniform deformation for the eight-layer nanobridge. While in uniform deformation the computational cell was exposed to a sequential increase of 1 Å in length at each step, in non-uniform deformation it was subjected to a initial increase of 1 Å for the first two steps and then a sudden increase of 16 Å at the third step that was followed by 2 and 5 Å increases in the subsequent steps. In the case of uniform deformation, the wire was broken at the 19th step. The non-uniform deformation, on the other hand, led to a complete formation of tubular structure: the transformation was initiated after the application of high-gradient stress—a sudden increase of 16 Å in length—and was finalized following the subsequent increments of 2 and 5 Å.

length of the computational cell— was perturbed by a sudden increase, varying from 5 to 20 Å, in the incremental step. In figure 2, we present the elongation processes for one set of simulations in both regimes.

From our extensive molecular static calculations, we found that the optimum length for the tubular structure was obtained when the nanobridge had eight layers of atoms along the axial direction. A brief discussion on this effect of the length on the formation of tubular structure will be given later in the text, but we now focus on the nature of the strain and its end effect in this specific transformation. Our calculations for the eight-layer nanobridge showed that linear deformation of neither low (1 or 2 Å increase in the length of the computational cell) nor high stress (incremental steps of 4, 5, and 6 Å in the length) determines the characteristics of this specific type of transformation, whereas when the nanowire is exposed to a suitable combination of low and high stresses (non-uniform deformation), the formation of tubular structure, initiated first at the ends and eventually completed in the middle, is observed[4]. It is important to note that not all combinations of low and high stress lead to complete transformation of the wire into a tubular structure.

In figure 3, we present snapshots of the observed structural transformation at various stages under a non-uniform deformation. On the right, snapshots of the cross-sectional view at respective stages are given. The first stage illustrates the relaxed geometry of the wire that was initially

[4] Supplementary material 1; movie showing the structural transformation under non-uniform deformation. (Available at stacks.iop.org/Nano/23/245707/mmedia).

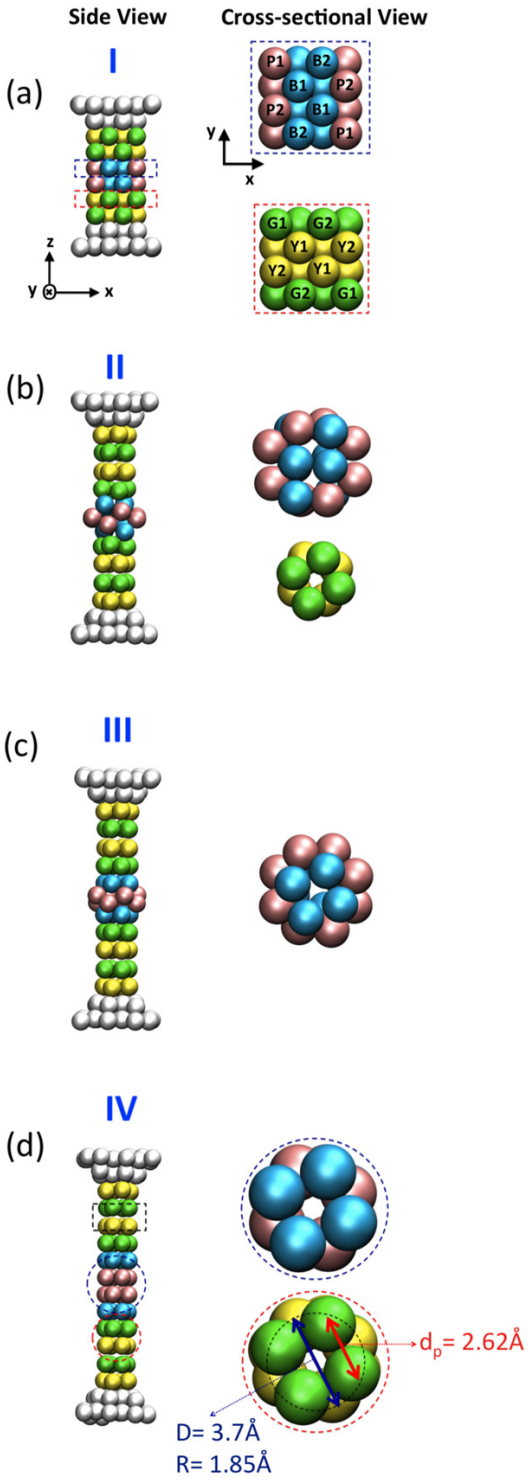

Figure 3. Snapshots of the structural transformation from a nanowire into a nanotube under non-uniform deformation: the left shows the side view and the right shows the cross-sectional view. The blue and pink colors represent the atoms in the nucleated region, whereas the yellow and green colors indicate the atoms closer to the ends. Relaxed configurations after each elongation mode: (a) low-stress elongation, (b) high-stress elongation, (c) low-stress elongation and (d) high-stress elongation. The rotational orientation of the layers closer to the ends (e.g. layers in the rectangularly framed region) is different from the ones in the more central region. In the last stage, d_p represents the length between atoms within the cross-sectional plane whereas D and R stand for the diameter and radius, respectively.

elongated by a total of 0.5 Å in length (total increment of 2 Å for the computational cell). The second stage, on the other hand, shows the atomic positions in the relaxed configuration after the wire was exposed to a much larger increase of 4.1 Å in length which amounts to a 16 Å increase in the length of the entire system (high-gradient stress). Upon application of high-gradient stress, the atomic rearrangements firstly appear at the center of the wire. During the process of energy minimization, both the top and the bottom layers of the wire (the darker atoms of the wire in figure 1) connecting the pins approach the adjacent pins and remain intact while the remaining layers split into two different layers containing four atoms. The subsequent two layers closer to the pins at both ends first split into two, thus initiating a symmetric tubular structure formation at both ends. In the meanwhile, nucleation takes place at the middle and with further non-uniform deformation (two subsequent increments of 0.07 Å and 0.18 Å in the interlayer separation which amount to 2 Å and 5 Å increase in the total length of the computational cell, respectively) the nucleated center also takes the tubular structure (see the third and fourth stages in figure 3). At the end of this sequential process, the entire nanowire transforms into a perfect nanotube with twelve layers of four atoms.

In figure 4, we illustrate the atomistic dynamics, at layers closer to the ends, in the process of geometric optimization at the second stage. The splitting of layers leading to the structural transformation from a wire to a tube can be clearly seen. In the relaxation procedure following the exposure to high-gradient stress, the downward movements of the yellow atoms are more or less equivalent, whereas the atomic arrangements of the green atoms are somewhat different in that splitting of the layer is firstly accompanied by upward motion of the G2 atoms and then followed by similar upward motion of the G1 atoms (see (b)–(d) in figure 4)[5]. As the single layer of the wire transforms into a two-layer hollow structure, both the yellow and the green atoms reorient themselves within their own plane in such a way that the respective orientation of the two newly formed planes is 45°, representative of the $4_A/4_B$ stacking suggested in [1]. This angular orientation is also followed when the dissociated layers are stacked along the axial direction to form the long tubular structure except for the two layers closer to the ends (see figure 5(a)). The nature of the structural evolution into tubular structure in the nucleated region shows similar characteristics: splitting of the layers is followed by in-plane atomic rearrangements leading to the formation of a square cross-sectional area.

The final geometry of the cross-sectional plane of the tubular structure is quite similar to that of a (4, 4) single wall silver nanotube (SWSNT) (see the cross-sectional view of the fourth stage in figure 3); the atomic positions of $4_A/4_B$ stacking form a circle with a radius of 1.85 Å which agrees well with the reported *ab initio* results of 1.80 Å [3] and 1.84 Å [14] for the (4, 4) SWSNT. The bond-length between

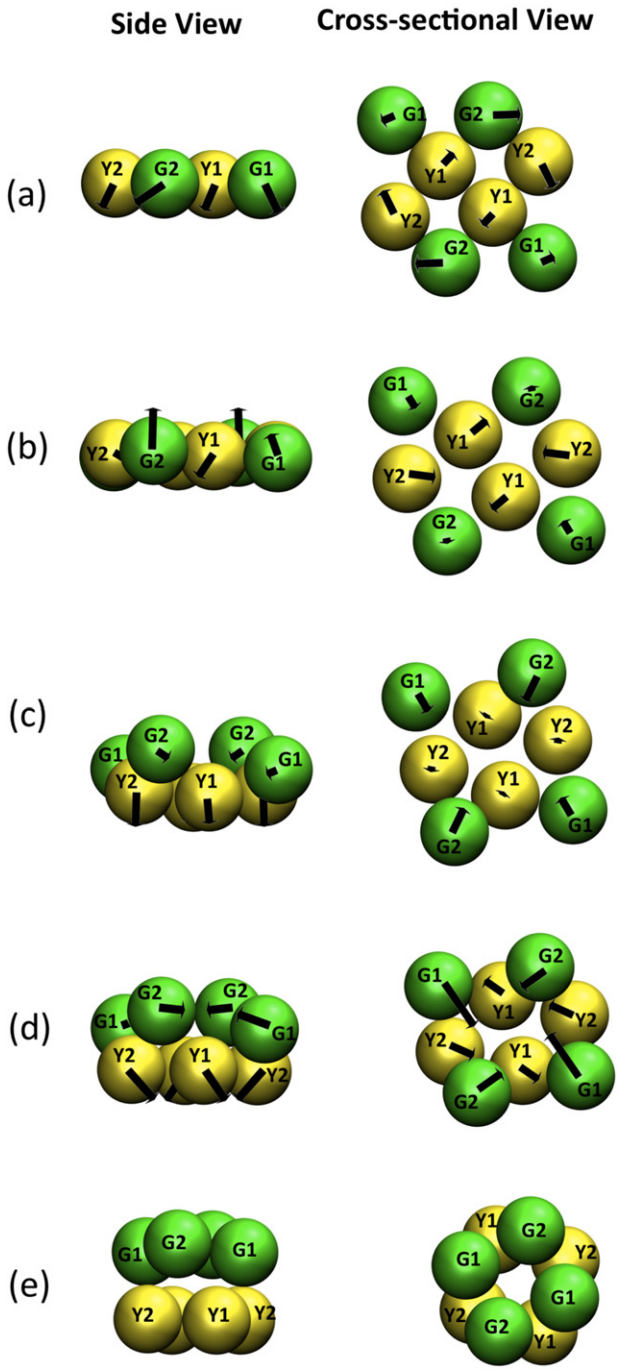

Figure 4. The atomic displacements leading to the tubular structure at stage II for the atoms closer to the ends of the nanobridge (the encircled green and yellow atoms in figure 3(a)).

two neighboring layers is 2.9 Å whereas the corresponding length between atoms within the same plane is 2.62 Å. It is also interesting to note that when the final nanotube is opened to form the respective sheet as shown in figure 5, the atomic arrangements comprise mostly a hexagonal structure with a horizontal length slightly shorter than the respective vertical length.

Although the effect of the length of the wire on the formation of the tubular structure was not investigated in the experiment, we think that it is an important issue to be

[5] Supplementary material 2; movie showing the splitting of a ⟨100⟩ layer into a two-layer hollow structure. (Available at stacks.iop.org/Nano/23/245707/mmedia).

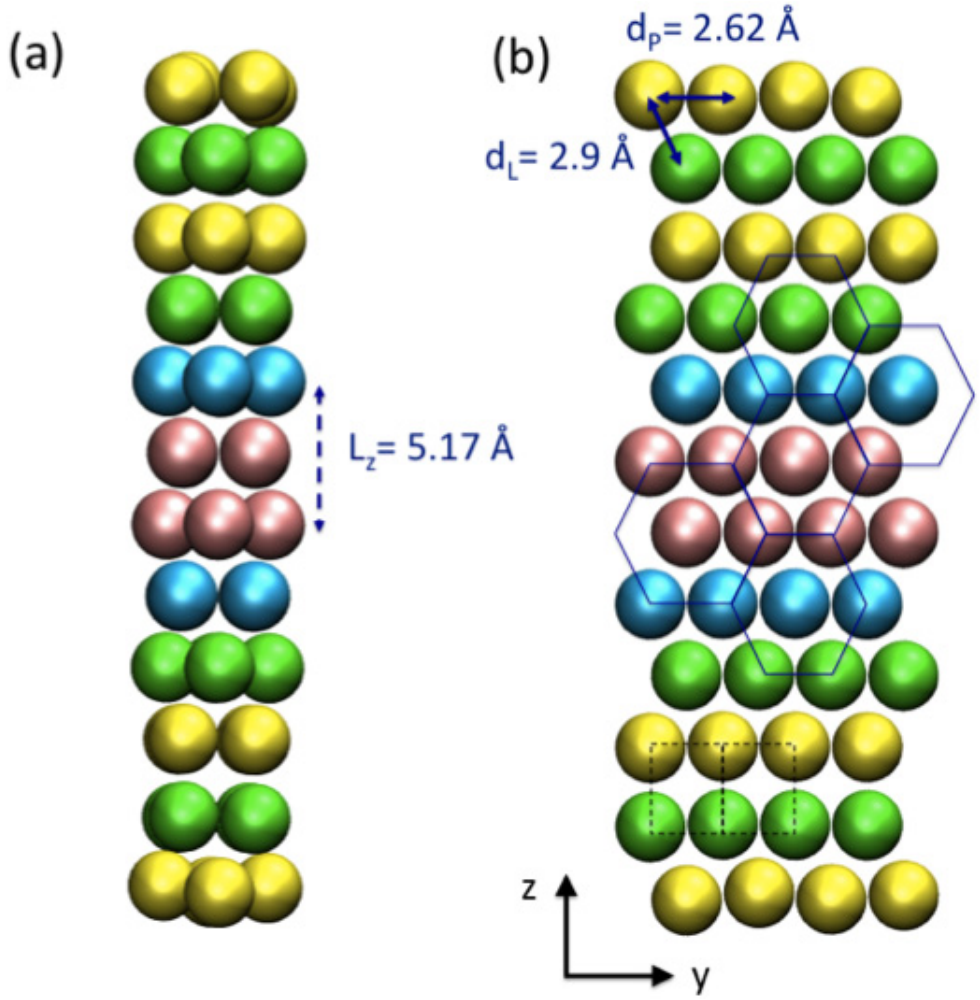

Figure 5. (a) Final form of the tubular structure, (b) planar view of the tube. Here, L_z, d_l, and d_p respectively stand for the length of the unit cell associated with the tubular structure, the bond-length between two neighboring layers, and the bond-length between atoms within the same plane.

addressed. We therefore performed extensive calculations on various nanobridges with different numbers of layers and presented the results in table 1. As is clearly seen in the table, a perfect and longest tube is obtained when the wire contains eight layers of atoms. During the procedure of energy minimization for all nanobridges with varying numbers of layers (n_w in table 1), both the top and the bottom layer attach to the neighboring pins and do not go through the splitting process; thus effectively leaving the wire with $(n_w - 2)$ layers that can transform into the tubular structure. Except for the nanowire with ten layers, all the wires underwent the expected structural transformation to a nanotube of $2(n_w - 2)$ layers. Our calculations further indicate that once this optimal length is exceeded, the wire easily breaks up under both forms of deformation: uniform and non-uniform. Let us recall that for longer nanowires (ten or more layers of wires) the tubular formation is always initiated but the wire is broken when it has a few layers of tubular geometry at the ends before completing the transformation into the middle. For the wire of ten layers, for example, the wire had four tubular layers at both ends before breaking up (figure 6). This is indeed not surprising when one looks at the nature of formation of the structural transformation: upon application of an appropriate set of strains the atoms at the ends of the wire first rearrange themselves to form a tubular structure whereas nucleation occurs at the center. With increasing length of wire, the region in which nucleation takes place extends from 3.92 Å for an eight-layer nanobridge to 12.93 Å for a 12-layer nanobridge. With the lengthy nucleated region, further strain is, obviously, needed to reassemble the nucleated atoms into a tubular structure. That further and stronger strain seems to exceed the threshold force that keeps the atoms together in the tubular structure, and thus leads to a breakdown of the wire at the ends.

We performed further calculations to explore the significance of the atomic arrangements within the cross-sectional plane of (100). Since our work was motivated by the experimental study on the formation of tubular structure with the smallest possible cross-section, we confined ourselves to nanowires of small cross-sectional area (see figure 7). Unlike the nanowire with the cross-sectional atomic arrangement in (b), neither the wire in (a) nor the wire in (c) went through a complete structural transformation from a wire to a tube before breaking up as the wire was exposed

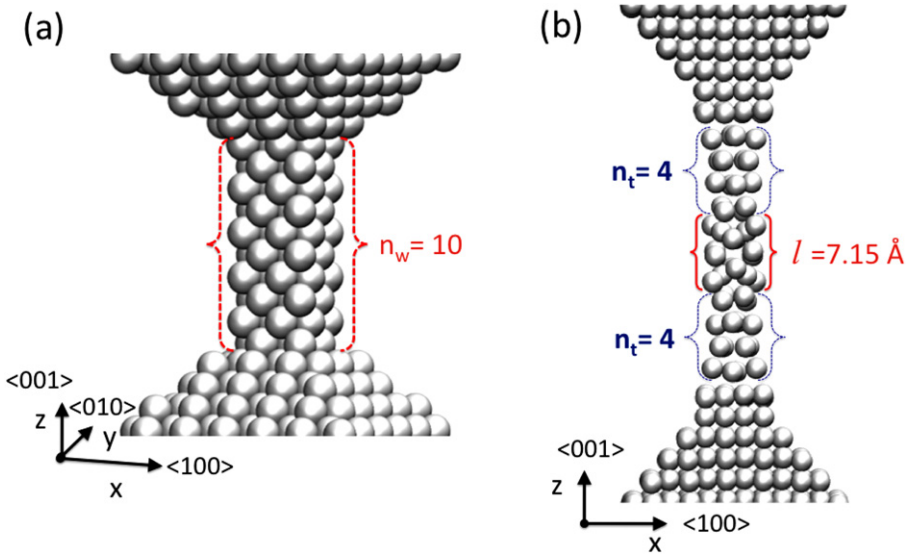

Figure 6. A ten-layer nanobridge: (a) before and (b) after exposure to the strain. l is the length of the nucleated region.

Table 1. The investigated nanobridges with the length ranging from four to ten layers. Here ΔL_z (Å) shows the total elongation on the nanobridge along the axial direction. The initial length is the length of the nanowire before the elongation process is started. The n_w and n_t columns indicate the number of layers in the initial nanowire and the obtained nanotube, respectively.

n_w	Initial length (Å)	ΔL_z (Å)	n_t
4	6.13	1.2	4
6	10.2	3.8	8
8	14.3	6.4	12
10	18.4	6.8	4

to a uniform/non-uniform strain. As can be easily seen in supplementary material II, available at stacks.iop.org/Nano/23/245707/mmedia, the atomic arrangement in (b) is best suited to initiate the formation of tubular structure: four atoms at the corners go up to form a four-atom layer of tubular structure whereas the remaining four atoms stay in the same plane to comprise the other layer of this specific structure. Furthermore, in the experimental work the authors also performed *ab initio* calculations on infinitely long nanowires with varying cross-sectional areas to support their experimental findings. They also found that nanowires with the specified atomic arrangement in the cross-sectional plane go through structural transformation which agrees well with our finding [1]. In addition, simulations using the MEAM potential on gold nanowires of finite length also showed a similar effect of the initial cross-sectional shape on the surface-stress-induced structural transformation [15].

To see the energetic response of the system to this specific type of structural transformation, we also computed the cohesive energies E_{coh} of the atoms taking a role in the process and plotted them in figure 8. The cohesive energy plot clearly reflects the progress in the structural transformation: throughout the entire process of elongation it is the second stage during which the cohesive energies of the Y1, Y2 and G1, G2 atoms for the first time converge to the same energies

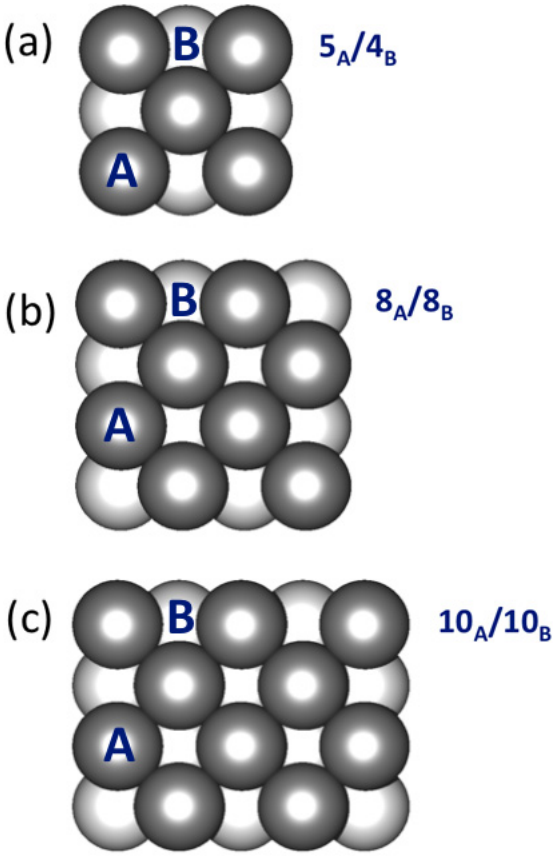

Figure 7. Atomic arrangements within the cross-sectional planes of the investigated nanowires. Each has AB stacking and varying number of atoms at each layer.

of −2.10 eV and −2.22 eV respectively, which is a strong indication of a new, symmetric in-plane atomic arrangement. On the other hand, during the same stage the atoms in the middle (P1, P2 and B1, B2) seem to be energetically independent, which is a clear sign of unsteadiness for this

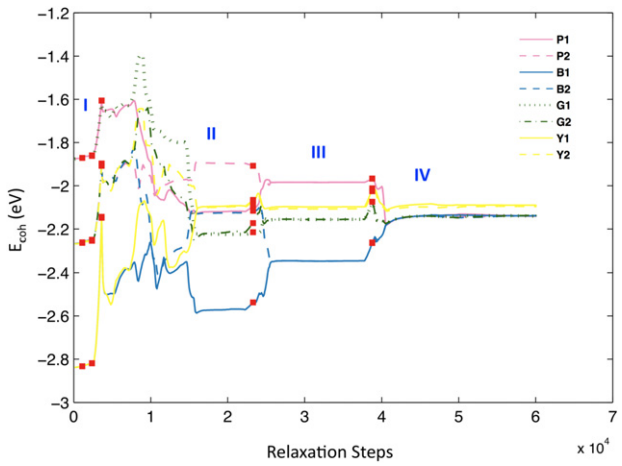

Figure 8. The cohesive energies for selected atoms (see figure 3) with respect to the relaxation steps in the entire process of elongation. The red squares indicate the points of axial elongation.

specific region. Upon further elongation, rearrangements of the atoms in the nucleated region towards a more stable configuration proceed (stage III). In the fourth stage during which the wire is exposed to first low then high stress the cohesive energies of most of the atoms of the wire finally converge to the same value of -2.14 eV which evidently represents a more stable structure. Even more interestingly, the distinct characteristic in the stacking of layers of the tubular structure can be clearly seen in the cohesive energy plot: the cohesive energy of the Y1 and Y2 atoms is somewhat different from those of the other atoms closer to the middle, reflecting the altered rotational orientation of the tubular layers closer to the ends of the wire (see (d) in figure 3).

4. Conclusion

In short, we have explored the atomistic nature of the spontaneous transformation of a silver nanowire into a nanotube under tensile stress and found that unless the nanowire is subject to a non-uniform deformation (a combination of low and high stresses), the atomic arrangements do not lead to a local minimum that specifies a nanotube with the smallest square cross-section. While the present molecular static calculations have provided further insights into the atomistic nature of the structural transformation, they also increase our need to understand the microscopic changes in the electronic structure and in the nature of the bonds between the atoms that are driven by the stretching of the wire. Thus, future work using *ab initio* electronic calculations will help us to further improve our understanding of the nature of this novel structural transformation. Furthermore, although the spontaneous formation of tubular structure was confirmed to be temperature independent in the experiment (the experiments were repeated at 150 and 300 K), the matter needs to be extensively investigated for a wide range of temperatures and molecular dynamic simulations along this line are on the way.

Acknowledgments

This work was supported by the Scientific and Technological Research Council of Turkey-TUBITAK under Grant No. 109T105. The computations were carried out through the National Center for High Performance Computing, located at Istanbul Technical University, under Grant No. 20132007. All the simulations were performed using the MD code LAMMPS [16] developed by Sandia National Laboratory.

References

[1] Lagos M J, Sato F, Bettini J, Rodrigues V, Galvaõ D S and Ugarte D 2009 *Nature Nanotechnol.* **4** 149
[2] Autreto P A S, Lagos M J, Sato F, Bettini J, Rocha A R, Rodrigues V, Ugarte D and Galvaõ D S 2011 *Phys. Rev. Lett.* **106** 065501
[3] Fa W, Zhou J, Dong J and Kawazoe Y 2011 *J. Chem. Phys.* **134** 244504
[4] da Silva E Z, da Silva A J R and Fazzio A 2001 *Phys. Rev. Lett.* **87** 256102
[5] Mehrez H and Ciraci S 1997 *Phys. Rev.* B **56** 12632
[6] Pauly F, Dreher M, Viljas J K, Häfner M, Cuevas J C and Nielaba P 2006 *Phys. Rev.* B **74** 235106
[7] Hasmy A, Rincón L, Hernández R, Mujica V, Márquez M and González C 2008 *Phys. Rev.* B **78** 115409
[8] Lee B-J, Shim J-H and Baskes M I 2003 *Phys. Rev.* B **68** 144112
[9] Foiles S M, Baskes M I and Daw M S 1986 *Phys. Rev.* B **33** 7983
[10] Baskes M I 1992 *Phys. Rev.* B **46** 2727
[11] Termentzidis K, Parasuraman J, da Cruz C A, Merabia S, Angelescu D, Marty F, Bourouina T, Kleber X, Chantrenne P and Basset P 2011 *Nanoscale Res. Lett.* **6** 288
[12] Ma F and Xu K W 2006 *J. Mater. Res.* **21** 2810
[13] Lee B-J, Wirth B D, Shim J-H, Kwon J, Kwon S C and Hong J H 2005 *Phys. Rev.* B **71** 184205
[14] Elizondo S L and Mintmire J W 2006 *Phys. Rev.* B **73** 045431
[15] Diao J, Gall K and Dunn M L 2003 *Nature Mater.* **2** 656
[16] Plimpton S 1995 *J. Comput. Phys.* **117** 1